● RESEARCH ARTICLE

Autologous nerve graft repair of different degrees of sciatic nerve defect: stress and displacement at the anastomosis in a three-dimensional finite element simulation model

Cheng-dong Piao[1], Kun Yang[2], Peng Li[3], Min Luo[4],[*]

1 Department of Orthopedics, Second Hospital, Jilin University, Changchun, Jilin Province, China
2 Basic Department, Air Force Aviation University of Chinese PLA, Changchun, Jilin Province, China
3 Department of Engineering Mechanics, Nanling Campus, Jilin University, Changchun, Jilin Province, China
4 Department of Pain, China-Japan Union Hospital, Jilin University, Changchun, Jilin Province, China

Correspondence to:
Min Luo, M.D., 2624500436@qq.com.

Abstract
In the repair of peripheral nerve injury using autologous or synthetic nerve grafting, the magnitude of tensile forces at the anastomosis affects its response to physiological stress and the ultimate success of the treatment. One-dimensional stretching is commonly used to measure changes in tensile stress and strain; however, the accuracy of this simple method is limited. Therefore, in the present study, we established three-dimensional finite element models of sciatic nerve defects repaired by autologous nerve grafts. Using PRO E 5.0 finite element simulation software, we calculated the maximum stress and displacement of an anastomosis under a 5 N load in 10-, 20-, 30-, 40-mm long autologous nerve grafts. We found that maximum displacement increased with graft length, consistent with specimen force. These findings indicate that three-dimensional finite element simulation is a feasible method for analyzing stress and displacement at the anastomosis after autologous nerve grafting.

Key Words: nerve regeneration; sciatic nerve injury; autologous nerve grafting; epineurial suturing; three-dimensional finite element models; load; stress; displacement; neural regeneration

Introduction

A number of studies have explored methods by which to assess peripheral nerve injury repair and associated biomechanical properties (Taylor et al., 2008; Cheng et al., 2009; Karabekmez et al., 2009; Alrashdan et al., 2010; di Summa et al., 2010; Dong et al., 2010; Ishiguro et al., 2010; Kadam et al., 2010; Szaro and Strong, 2010; Vinik, 2010; Bielle et al., 2011; Chen et al., 2011; Dadon-Nachum et al., 2011; Korte et al., 2011; Ngeow et al., 2011; Wolford and Rodrigues, 2011; Unni et al., 2012). Wang et al. (2009) confirmed that catheters synthetized from polycaprolactone and dimethyl fumarate were strong and showed good histocompatibility, and successfully promoted differentiation and regeneration of Schwann cells in rats with 10-mm sciatic nerve defects; good growth was observed by 6 weeks after grafting. Regeneration of the sciatic nerve was demonstrated 1 month after insertion of an artificial catheter made from nanosilver and type I collagen to repair a 10-mm sciatic nerve defect; retrograde tracing showed regenerating neurons in the dorsal root gan-glion, and good electrophysiological function was observed (Ding et al. 2010). In a 10-mm sciatic nerve injury in fresh human tissue, Peng et al. (2012) showed that maximum tensile load, displacement, stress and strain were lower after repair using a multilayer curled amniotic tube than after autologous nerve anastomosis. Ngeow et al. (2011) confirmed that compound action potential was notably improved at 6 weeks, and recovery of gait function was good at 12 weeks, in animals with sciatic nerve injury after epineurial suturing.

In the repair of peripheral nerve injury using autologous or synthetic nerve grafts, the magnitude of tension at the anastomosis is a crucial factor influencing the response of the graft to physiological stress and the success of the treatment. In previous studies, tension at the anastomosis under physiological load has commonly been measured using one-dimensional stretching (Wang et al., 2009; Peng et al., 2012). However, such techniques measure the tension across the whole specimen, rather than specifically at the anastomosis. Computer simulation can be used to create
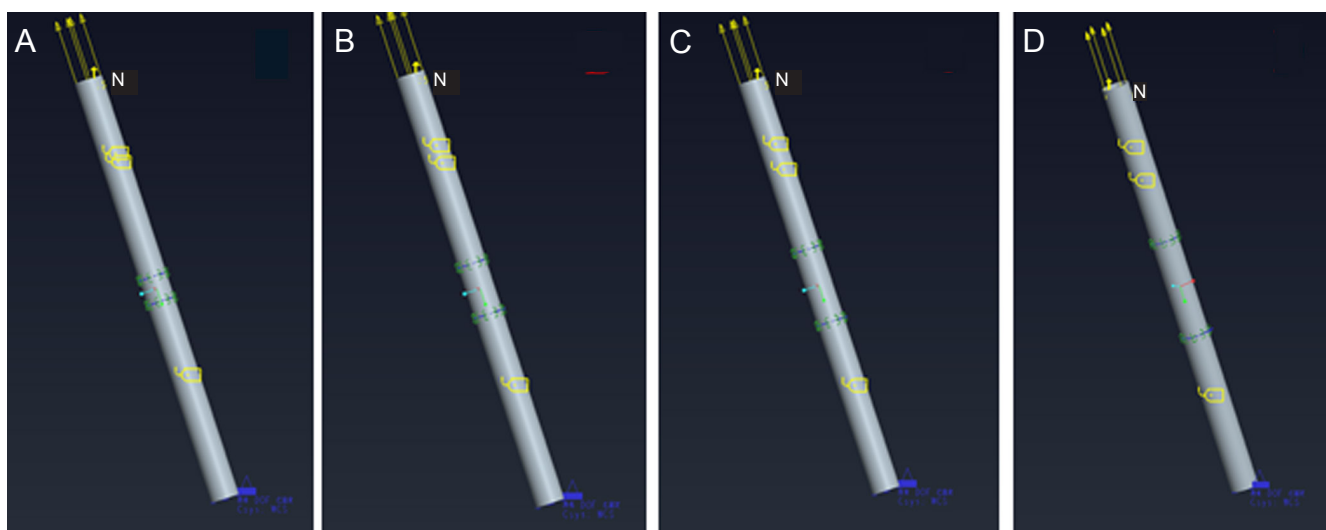
Figure 1 Three-dimensional models of sciatic nerve injury repaired by autologous nerve grafting.
(A–D) Models of 10- (A), 20- (B), 30- (C), and 40-mm (D) long autologous nerve grafts. Yellow arrows represent tension; yellow line and point represent node; black represents tetrahedral element made by node connection; N represents load.
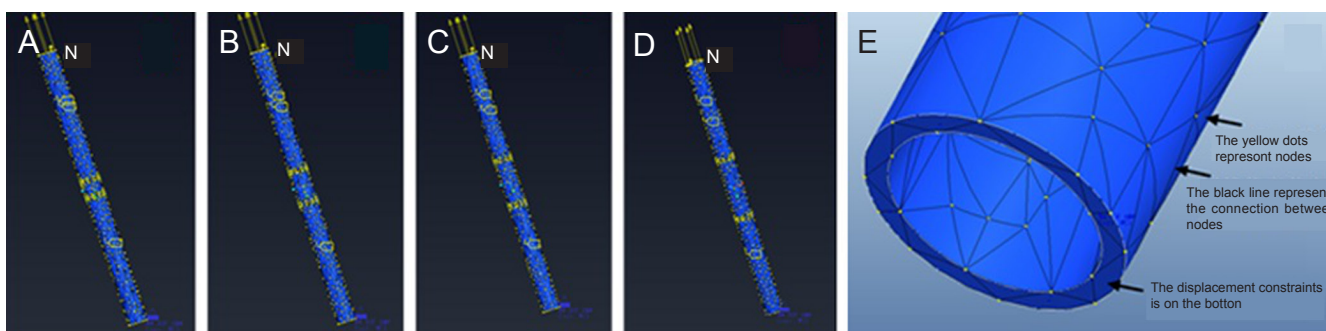

Figure 2 Grid graphs of three-dimensional finite element models of sciatic nerve injury repaired by autologous nerve grafting.
(A–D) Grid graphs of models of 10- (A), 20- (B), 30- (C) and 40-mm (D) long autologous nerve grafts. (E) Tetrahedral elements and grid amplification. Displacements of the base was restricted. Yellow arrows represent tension; yellow point represents node; black lines represent node connection; N represents load.
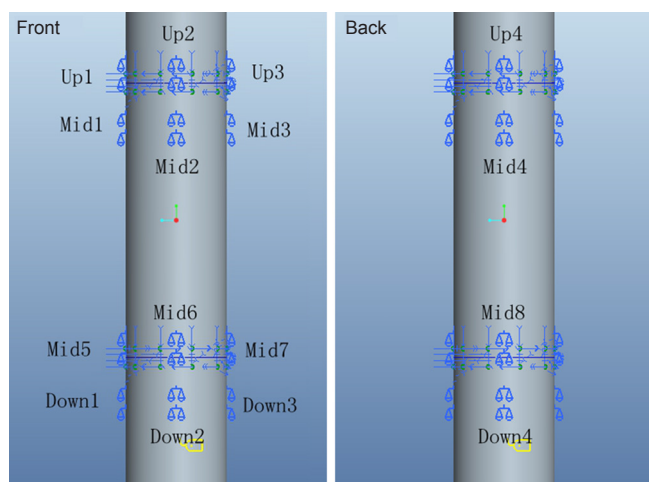

Figure 3 Positions of the measurement points in the three-dimensional finite element simulation model of sciatic nerve injury repaired by autologous nerve grafting.
Four equally-spaced measuring points were set along the circumference at the upper and lower edges of the anastomosis at either end of the model, *i.e.*, 16 measurement points per model.

a three-dimensional (3D) model using the finite element method. This can be used to calculate the tension and deformation at the edge of a simulated anastomosis under physiological load, and to directly and precisely identify the mechanical properties at its edge. Thus, the technique has clinical value in sciatic nerve injury grafts.

We established 3D finite element models of sciatic nerve defects repaired by different lengths of autologous nerve grafts, and used them to calculate the stress and displacement at the anastomosis. Here, we provide a simulated modeling and calculation method for exploring grafting and repair of sciatic nerve injury in the clinic.

Materials and Methods

Establishment of 3D finite element models of sciatic nerve injury repaired by autologous nerve grafting

Small deformations of the sciatic nerve are elastic (Peng et al., 2012). More precisely, the sciatic nerve is a viscoelastic material, but at present it is difficult to model as such. Therefore, to simplify the calculation process, we assume here that

Table 1 Maximum stress (MPa) and maximum displacement (mm) in the three-dimensional finite element simulation model of sciatic nerve injury repaired by autologous nerve grafts of various lengths

Measuring point	10-mm autologous nerve grafting group		20-mm autologous nerve grafting group		30-mm autologous nerve grafting group		40-mm autologous nerve grafting group	
	$\sigma1$	Y displacement	$\sigma1$	Y displacement	$\sigma1$	Y displacement	$\sigma1$	Y displacement
Up1	0.1388	0.5417	0.1339	0.5653	0.1247	0.5699	0.1432	0.5978
Up2	0.1252	0.7060	0.1257	0.6940	0.1280	0.7435	0.1251	0.7722
Up3	0.1049	0.7731	0.0852	0.7886	0.1208	0.8097	0.1096	0.8612
Up4	0.1365	0.6067	0.1672	0.6122	0.1471	0.6286	0.1625	0.6761
Mid1	0.1516	0.4388	0.1454	0.4611	0.1345	0.4789	0.1438	0.4996
Mid2	0.1020	0.4444	0.1240	0.4583	0.1311	0.4762	0.1092	0.5065
Mid3	0.1221	0.4444	0.1036	0.4661	0.0917	0.4857	0.0898	0.5210
Mid4	0.1463	0.4492	0.1260	0.4672	0.1557	0.4879	0.1544	0.5106
Mid5	0.1741	0.4236	0.1661	0.4076	0.1687	0.3861	0.1791	0.3675
Mid6	0.1270	0.4310	0.1269	0.4051	0.1259	0.3845	0.1392	0.3768
Mid7	0.2033	0.4427	0.1679	0.4091	0.1553	0.3907	0.1527	0.3878
Mid8	0.1264	0.4342	0.1371	0.4125	0.1263	0.3941	0.1530	0.3771
Down1	0.1618	0.2983	0.1686	0.2795	0.1697	0.2601	0.1612	0.2405
Down2	0.1191	0.2960	0.1027	0.2768	0.1136	0.2578	0.1376	0.2382
Down3	0.1501	0.2975	0.1577	0.2783	0.1416	0.2594	0.1243	0.2387
Down4	0.1005	0.2971	0.1321	0.2774	0.1099	0.2573	0.1319	0.2388

$\sigma1$: Maximum stress; Y displacement: maximum longitudinal displacement.

the sciatic nerve is a thin-walled incompressible isotropic elastic tube.

We used the average dimensions of the gluteus maximus segment of the sciatic nerve in the Chinese population (length, 170 mm; outer diameter, 11 mm; inner diameter, 9 mm; Yan and Huang, 1998) as input parameters for PRO E 5.0 finite element analysis software (Parametric Technology Corporation, Needham, MA, USA) and produced 3D finite element models of sciatic nerve injury repaired by 10, 20, 30, and 40-mm autologous nerve grafts (**Figure 1**).

Grid scheduling analysis and optimization were conducted in the models, which were meshed using PRO E 5.0. There were 4,901 tetrahedral elements in the 10-mm long graft models, 5,614 in the 20-mm long models, 5,492 in the 30-mm long models, and 6,045 in the 40-mm long models (**Figure 2**).

A 5 N load was applied to the models, and PRO E 5.0 was used to calculate the stress and displacement at each element and node.

Boundary condition
A fixed constraint was used in each anastomosis at the distal end of the sciatic nerve injury models (**Figure 1**). Only the sciatic nerve was included in the finite element calculation. The elastic modulus of the sciatic nerve was E = 40.96 ± 2.59 MP (Liu et al., 2012). The stress at each node was calculated according to Hooke's law, $\sigma = E\varepsilon$ (where σ = stress, E = elastic modulus, and ε = strain) (Liu, 1979).

Measurement points
Epineurial suturing was simulated in the models. Four measurement points were set at equal distances along the circumference at the upper and lower edges of the anastomosis, at each end of the model, *i.e.*, 16 measurement points per model (**Figure 3**).

Statistical analysis
Data are expressed as the mean ± SD, and were analyzed using SPSS 16.0 software (SPSS, Chicago, IL, USA). One-way analysis of variance and Scheffe's method were used to determine the significance of intergroup differences, and $P < 0.05$ was considered statistically significant.

Results
Under a 5 N load, the maximum displacement was found at measurement point 3 in the upper segment of the graft (designated Up3; **Figure 3**) in all four models. The largest maximum displacement was observed in the 40-mm long model, followed by 30- and 20-mm long models, and the smallest in the 10-mm long model ($P < 0.05$). That is, the longer the graft, the larger the displacement under the same load, consistent with mechanical laws. These data indicate that the simplification used in our 3D finite element model resulted in a reasonable simulation of sciatic nerve injury (**Table 1**).

Discussion
The key to 3D finite element modeling is simplifying complex mechanical systems. Here, the sciatic nerve is considered to be a thin-walled elastic cylinder. The simplification of 3D finite element models used in the present simulation of sciatic nerve injury resulted in a reasonable representation of the mechanics of this complex system, and advanced PRO E 5.0 software was used to calculate the stress and displacement of each element and node under a 5 N load and uniaxial tension, providing reliable experimental results.

The magnitude of tensile forces at the anastomosis under physiological stress is an important factor influencing the outcome of peripheral nerve injury repair after suturing (Yan and Huang, 1998). Our results demonstrated that under a 5 N

load, the maximum displacement appeared at measurement point Up3 in all four autologous nerve grafts, showing good consistency across the models. Up3 lies at the right-hand upper edge of the proximal end of the anastomosis, and very near to the loading point, so its displacement is large. Under the same load, the maximum stress and displacement correlate with the length of the graft. Our data are in accordance with the specimen force law and comparable with results from previous studies, indicating that the present study design and mechanical simplification are reasonable representations of the system modeled.

Previous studies have demonstrated that the tension and elongation of the anastomosis after injury to peripheral nerves such as the sciatic nerve are commonly measured by simple electrical measurement of stretch and strain at the site of the anastomosis (Yan and Huang, 1998; Ngeow et al., 2011). For example, Liu et al. (2012) used electrical measurement to determine the tensile forces at various points on a sciatic nerve anastomosis after perineurial or epineurial suturing, but used only a 10-mm long autologous nerve graft and one-dimensional tension. The present study is more representative of clinical practice, because we used 3D finite element models of sciatic nerve injury repaired by autologous nerve grafts of different lengths to calculate the stress and displacement at the anastomosis.

In conclusion, our results demonstrate the feasibility of using a 3D finite element simulation model of sciatic nerve injury to predict anastomosis stress and displacement after autologous nerve grafting.

References

Alrashdan MS, Park JC, Sung MA, Yoo SB, Jahng JW, Lee TH, Kim SJ, Lee JH (2010) Thirty minutes of low intensity electrical stimulation promotes nerve regeneration after sciatic nerve crush injury in a rat model. Acta Neurol Belg 110:168-179.

Bielle F, Marcos-Mondéjar P, Leyva-Díaz E, Lokmane L, Mire E, Mailhes C, Keita M, García N, Tessier-Lavigne M, Garel S, López-Bendito G (2011) Emergent growth cone responses to combinations of Slit1 and Netrin 1 in thalamocortical axon topography. Curr Biol 21:1748-1755.

Chen Z, Lu XCM, Shear DA, Dave JR, Davis AR, Evangelista CA, Duffy D, Tortella FC (2011) Synergism of human amnion-derived multipotent progenitor (AMP) cells and a collagen scaffold in promoting brain wound recovery: Pre-clinical studies in an experimental model of penetrating ballistic-like brain injury. Brain Res 1368:71-81.

Cheng FC, Tai MH, Sheu ML, Chen CJ, Yang DY, Su HL, Ho SP, Lai SZ, Pan HC (2009) Enhancement of regeneration with glia cell line-derived neurotrophic factor-transduced human amniotic fluid mesenchymal stem cells after sciatic nerve crush injury. J Neurosurg 112:868-879.

Dadon-Nachum M, Sadan O, Srugo I, Melamed E, Offen D (2011) Differentiated mesenchymal stem cells for sciatic nerve injury. Stem Cell Rev 7:664-671.

di Summa PG, Kingham PJ, Raffoul W, Wiberg M, Terenghi G, Kalbermatten DF (2010) Adipose-derived stem cells enhance peripheral nerve regeneration. J Plast Reconstr Aesthet Surg 63:1544-1552.

Ding T, Luo ZJ, Zheng Y, Hu XY, Ye ZX (2010) Rapid repair and regeneration of damaged rabbit sciatic nerves by tissue-engineered scaffold made from nano-silver and collagen type I. Injury 41:522-527.

Dong W, Chen H, Yang X, Guo L, Hui G (2010) Treatment of intracerebral haemorrhage in rats with intraventricular transplantation of human amniotic epithelial cells. Cell Biol Int 34:573-577.

Ishiguro M, Ikeda K, Tomita K (2010) Effect of near-infrared light-emitting diodes on nerve regeneration. J Orthop Sci 15:233-239.

Kadam SS, Sudhakar M, Nair PD, Bhonde RR (2010) Reversal of experimental diabetes in mice by transplantation of neo-islets generated from human amnion-derived mesenchymal stromal cells using immuno-isolatory macrocapsules. Cytotherapy 12:982-991.

Karabekmez FE, Duymaz A, Moran SL (2009) Early clinical outcomes with the use of decellularized nerve allograft for repair of sensory defects within the hand. Hand (N Y) 4:245-249.

Korte N, Schenk HC, Grothe C, Tipold A, Haastert-Talini K (2011) Evaluation of periodic electrodiagnostic measurements to monitor motor recovery after different peripheral nerve lesions in the rat. Muscle Nerve 44:63-73.

Liu GY, Zhang Q, Jin Y, Gao ZL (2012) Stress and strain analysis on the anastomosis site sutured with either epineurial or perineurial sutures after simulation of sciatic nerve injury. Neural Regen Res 7:2299-2304.

Liu HW (1979) Material Mechanics. Beijing: People's Education Press.

Ngeow WC, Atkins S, Morgan CR, Metcalfe AD, Boissonade FM, Loescher AR, Robinson PP (2011) The effect of Mannose-6-Phosphate on recovery after sciatic nerve repair. Brain Res 1394:40-48.

Peng CG, Zhang Q, Yang Q, Zhu QS (2012) Strain and stress variations in the human amniotic membrane and fresh corpse autologous sciatic nerve anastomosis in a model of sciatic nerve injury. Neural Regen Res 7:1779-1785.

Szaro BG, Strong MJ (2010) Post-transcriptional control of neurofilaments: New roles in development, regeneration and neurodegenerative disease. Trends Neurosci 33:27-37.

Taylor CA, Braza D, Rice JB, Dillingham T (2008) The incidence of peripheral nerve injury in extremity trauma. Am J Phys Med Rehabil 87:381-385.

Unni DK, Piper M, Moldrich RX, Gobius I, Liu S, Fothergill T, Donahoo A-LS, Baisden JM, Cooper HM, Richards LJ (2012) Multiple Slits regulate the development of midline glial populations and the corpus callosum. Dev Biol 365:36-49.

Vinik A (2010) The approach to the management of the patient with neuropathic pain. J Clin Endocrinol Metab 95:4802-4811.

Wang S, Yaszemski MJ, Knight AM, Gruetzmacher JA, Windebank AJ, Lu L (2009) Photo-crosslinked poly(ε-caprolactone fumarate) networks for guided peripheral nerve regeneration: Material properties and preliminary biological evaluations. Acta Biomaterialia 5:1531-1542.

Wolford LM, Rodrigues DB (2011) Autogenous grafts/allografts/conduits for bridging peripheral trigeminal nerve gaps. Atlas Oral Maxillofac Surg Clin North Am 19:91-107.

Yan QS, Huang YT (1998) Applied anatomy of sciatic nerve in hips. Ningxia Yixue Zazhi 20:162-164.